JACS
JOURNAL OF THE AMERICAN CHEMICAL SOCIETY
Article
pubs.acs.org/JACS

BH_3 under Pressure: Leaving the Molecular Diborane Motif

Yansun Yao[†] and Roald Hoffmann*[,‡]

[†]Steacie Institute for Molecular Sciences, National Research Council of Canada, Ottawa, ON, K1A 0R6 Canada
[‡]Department of Chemistry and Chemical Biology, Cornell University, Baker Laboratory, Ithaca, New York 14853, United States

Supporting Information

ABSTRACT: Molecular and crystalline structures of $(BH_3)_n$ have been theoretically studied in the pressure regime from 1 atm to 100 GPa. At lower pressures, crystals of the familiar molecular dimer are the structure of choice. At 1 atm, in addition to the well-characterized β diborane structure, we suggest a new polymorph of B_2H_6, fitting the diffraction lines observed in the very first X-ray diffraction investigation of solid diborane, that of Mark and Pohland in 1925. We also find a number of metastable structures for oligomers of BH_3, including cyclic trimers, tetramers, and hexamers. While the higher oligomers as well as one-dimensional infinite chains (bent at the bridging hydrogens) are less stable than the dimer at ambient pressure, they are stabilized, for reasons of molecular compactness, by application of external pressure. Using periodic DFT calculations, we predict that near 4 GPa a molecular crystal constructed from discrete trimers replaces the β diborane structure as the most stable phase and remains as such until 36 GPa. At higher pressures, a crystal of polymeric, one-dimensional chains is preferred, until at least 100 GPa.

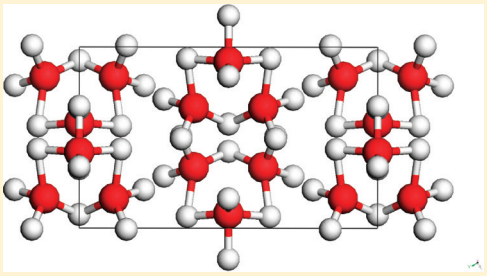

INTRODUCTION

Diborane, B_2H_6, **1**, is the prototypical electron-deficient molecule. Understanding the bonding in diborane was an important step in the extension of molecular orbital ideas to both electron-poor and electron-rich nonoctet molecules.[1−4] In this paper, we take diborane theoretically into the realm of high pressure, complementing previous experimental[5] and theoretical studies.[6,7] As we will see, interesting structural alternatives to B_2H_6, ones one might have considered even at ambient conditions, come to the fore, and something is learned about diborane itself.

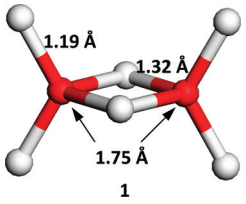

1

B_2H_6 solidifies at 108 K. At least four crystalline forms of diborane appear in the literature, with a pivotal state single crystal structure determination of one of them. As early as 1925, on the basis of the powder diffraction pattern, Mark and Pohland reported a crystalline phase of B_2H_6 in liquid air, assigned four B_2H_6 molecules to an orthohexagonal unit cell, got an approximate B−B separation (1.8−1.9 Å), but could not obtain the atomic positions.[8] The double-bridging structure of the B_2H_6 molecule was not known at that time. In 1959, Bolz, Mauer, and Peiser[9] reported two crystalline phases of B_2H_6 in the temperature region from 4.2 to 100 K, naming them α and β. The α phase was formed by deposition from gaseous B_2H_6 at 4.2 K. It transformed slowly to the β phase above 60 K, which in turn was obtained by deposition at 77 K and annealing to 90 K. Interestingly, neither of the α and β phases nor the additional phase found by passing B_2H_6 through a microwave discharge showed a diffraction pattern that corresponded to the phase reported earlier by Mark and Pohland. The refinement of the diffraction data for the three phases they found, was, however, not carried out by Bolz, Mauer, and Peiser.

In 1965, using single-crystal X-ray diffraction, Smith and Lipscomb[10] successfully characterized the β phase in atomic detail. The structures of all other crystalline phases of B_2H_6 remain unknown; we will have a suggestion for one of them. The β phase is monoclinic (space group $P2_1/n$, $Z = 2$, $a = 4.40$, $b = 5.72$, $c = 6.50$ Å, and $\gamma = 105.1°$). The metrics of **1** shown above come from the Smith and Lipscomb structure; the known difficulties with locating hydrogens by X-ray diffraction should be kept in mind. The structure of the molecule in the gas phase is also available from electron diffraction (an interesting story in itself[11]) and strong evidence for it from infrared spectroscopy.[12]

METHODS

Gas phase structural optimizations and energy evaluations were performed using valence double/triple-ζ plus polarization (cc-pVDZ and cc-pVTZ) basis set.[13] All predicted molecules were optimized at the correlated single-reference MP2 level, and confirmed as minima or saddle points using harmonic vibrational analysis. Correlation effects beyond the MP2 level were estimated via single-point CCSD(T) calculations using both cc-pVDZ and cc-pVTZ basis sets. The zero-point vibrational corrections (zero-point energy, ZPE) were determined at the MP2 level using both cc-pVDZ and cc-pVTZ

Received: October 8, 2011
Published: November 21, 2011

   dx.doi.org/10.1021/ja2092568 | J. Am. Chem.Soc. 2011, 133, 21002−21009

basis sets, and calculated from the harmonic vibrational frequencies. All molecular calculations were performed using GAMESS-US.[14]

Solid-state structural optimizations and energy calculations were performed using plane-wave/pseudopotential density function theory (DFT) methods. The VASP program[15] was implemented with the projected augmented wave (PAW) potential,[16] the Perdew–Burke–Ernzerhof (PBE) exchange-correlation functional,[17] and a kinetic energy cutoff of 910 eV. The Monkhorst-Pack (MP) k-point mesh[18] were used to sample the first Brillouin zone (BZ), scaled according to the reciprocal-lattice vectors with a basic division of 8. The electronic self-consistency loops were stopped when the total energy change between two steps are less than 10^{-7} eV. Structural relaxation loops were continued until the Hellmann–Feynman force on each atom became smaller than 0.001 eV/Å. Solid-state phonon calculations were performed using the ABINIT program,[19] employing the linear response method, Trouiller-Martins-type[20] pseudopotentials with an energy cutoff of 35 hartree, and the PBE exchange-correlation functional. A $4 \times 4 \times 4$ q-point mesh was used for BZ sampling. At each q point, the dynamical matrix was calculated with an $8 \times 6 \times 4$ and $4 \times 8 \times 6$ k-point mesh for the P-1 (trimer) and $P2_1/c$ (2) structure (see below), respectively.

Crystal structures were constructed in two steps: (1) searching for the most stable isomers with the stoichiometry 1B:3H and (2) searching for the optimal stacking patterns for the isomers. For each type of molecule/chain, several trial structures were set up, making an educated guess of the boron framework and placing the H atoms at a set of available positions in the boron framework. The trial molecules generated were fully optimized and the lowest energy ones were selected for vibrational analysis. Multiple stacking patterns were generated in unit cells that contain up to two molecules/chains, adopting either symmetrical or triclinic lattices with arbitrary cell shapes.

The trial crystal structures were fully optimized and candidates with the lowest enthalpies were selected. To make sure that the selected crystalline structures indeed correspond to local energy minima, each structure was annealed to 300 K and equilibrated for 10 ps, using a molecular dynamics (MD) simulation in NVT ensemble, followed by a second structural optimization. In the MD annealing simulations, the VASP program and same potentials as described above were used. MD trajectories were sampled with a 1 fs time interval. The annealed structures were then compared with the original ones to examine possible structural changes. Sometimes new structures were produced in this annealing procedure. The structural searches have been performed at five pressures, 1 atm, 10 GPa, 20 GPa, 50 GPa, and 100 GPa, in order to obtain a complete spectrum of the most stable crystalline structures of B_2H_6 in different pressure regions.

RESULTS AND DISCUSSION

Alternatives for Diborane. As the name implies, diborane is a dimer of the known BH_3, a D_{3h} molecule kinetically unstable to dimerization. The dimerization equilibrium is shifted to the monomer side in BX_3, X = halogen and other lone pair bearing groups, for well-understood π-bonding reasons.[21]

Other structures for $(BH_3)_n$ come from theory, not from experiment. These include trimers and tetramers, molecules **2** and **3**. One can also think of (though these have not been written down in the literature, as far as we know) higher rings (we show the six-membered ring, **4**) as well as a polymeric chain **5**. The general analogy of $(CH_2)_n$ and $(BH_3)_n$ structures is obvious; we will come back to it later.

A word about the representations here: There is no universally accepted notation for electron-deficient three-center bonds, open or closed.[1] The notation we use is imperfect; the two lines drawn to a bridging hydrogen do *not* represent two two-electron bonds, but together stand for an open three-center two-electron bond. Also, the structural drawings just indicate bonding, carrying no three-dimensional geometrical implication. As we will see, all these molecules are nonplanar, with bent BHB bridges.

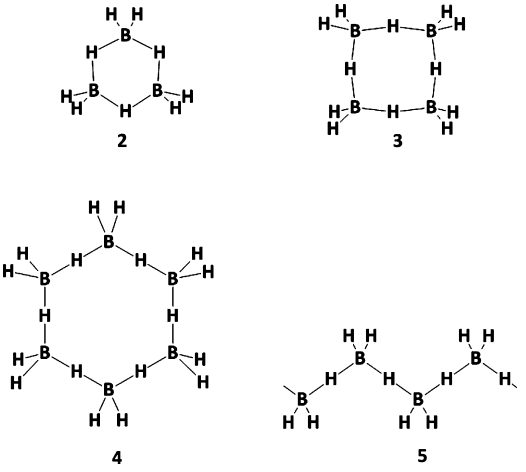

Note that the same simple electron-poor three-center bond ideas that go into the simplest description of a diborane allow a satisfactory first description of **2**–**5** as well.

Solid Diborane at Ambient Pressure. Theory gives several interesting structures for B_2H_6 at 1 atm, all built up from D_{2h} dimers and differing only in their stacking. Not surprisingly, these structures have very similar calculated energies at 1 atm. The DFT implementation used by us (see the Methods section) has well-known deficiencies in treating dispersive interactions, so at low pressures we expect moderate deviations of calculated energies, force constants, and structural parameters from the experimental values. Among the low energy structures at 1 atm, we found the β diborane structure characterized by Smith and Lipscomb, as well as several new structures in the same space group ($P2_1/c$, equivalent to $P2_1/n$). One of these newly predicted structures, denoted as $P2_1/c$ (1) (structural details in the Supporting Information (SI)), has interplanar spacings that can reasonably reproduce the diffraction lines of the crystalline phase reported by Mark and Pohland. The $P2_1/c$ (1) structure adopts a monoclinic unit cell (Figure 1) rather than the suggested orthohexagonal unit cell,

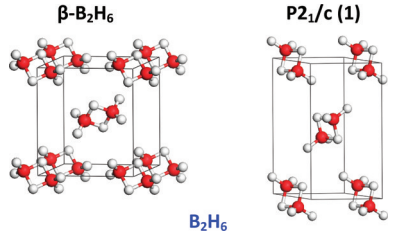

Figure 1. Selected solid diborane structures.

but is very close to the latter. The optimized lattice parameters for the $P2_1/c$ (1) structure are a = 4.46, b = 8.68, c = 4.55 Å, and β = 120.5°, in good agreement with the lattice parameters suggested by Mark and Pohland, a = 4.54, b = 4.54, c = 8.69 Å, and γ = 120.0° (in a hexagonal setting; in the transformation between monoclinic and hexagonal cells, the lattice vectors b and c are exchanged).

The simulated diffraction pattern for the $P2_1/c$ (1) structure is consistent with the measured pattern (SI). Indeed, except for one missing peak, from the 121 reflection, all the experimental

dx.doi.org/10.1021/ja2092568 | J. Am. Chem.Soc. 2011, 133, 21002–21009

diffraction peaks can be indexed with the $P2_1/c$ (1) structure. In terms of stacking, the $P2_1/c$ (1) structure is less efficient than the β phase, which results into a larger volume for the $P2_1/c$ (1) structure (which then destabilizes it rapidly at the high pressures we will study next). We are thus making a prediction here of the $P2_1/c$ (1) structure for the Mark and Pohland phase.

Because the structural information available is insufficient, we have not attempted to solve the crystalline structure of the α phase of Bolz, Mauer, and Peiser. Powder patterns indicated that the α phase is closely related to the β phase, and coexists with the latter over a considerable range of temperature,[9] which makes an unambiguous identification of the α phase difficult. The various molecular diborane structures we found, including β diborane and the $P2_1/c$ (1) structure, are all within 5 meV/molecule of each other in our calculations at P = 1 atm. So it is no surprise that there are several polymorphs of diborane.

We hope these considerations will encourage further experimental study of B_2H_6 at low temperatures; it would be good to straighten out the story of the four phases in the literature.

Other $(BH_3)_n$ Structures. The only imperative as high pressure is applied, for instance, in a diamond anvil cell, is "get denser". This is achieved by a progression of squeezing out van der Waals space, rearrangement to more compact isomers of a molecule, and eventually increasing stepwise coordination of all atoms.[22] It is this increasing compactness that led us to think of the trimers, tetramers, and higher oligomers of diborane. We consider in this paper a trimer (B_3H_9), tetramer (B_4H_{12}), and hexamer (B_6H_{18}), as well as infinite 1-D chains, all with the stoichiometry 1B:3H.

Several theoretical models have already been proposed for the structure of the B_3H_9 molecule. A D_{3h} structure with all bridging H atoms in the plane of B atoms corresponds to a saddle point with three imaginary modes.[23] Previous studies[24,25] suggest that a cyclic C_{3v} structure (Figure 2), with all bridging H atoms above the plane of B atoms, is more stable than all acyclic structures.[26] Our calculations agree. The C_{3v} trimer, however, is less stable per BH_3 (at 1 atm) than the D_{2h} diborane dimer. Taking the C_{3v} trimer, if one moves one bridging H atom below the plane of B atoms and reoptimizes the structure, one obtains another isomer, C_s in symmetry (minimum confirmed by a vibrational analysis). The energy of the C_s dimer is slightly higher than that of the C_{3v} trimer, by 0.011 eV/BH_3 (at CCSD(T)/cc-pVTZ level, see SI to this paper). A pentacoordinated "open" C_2 trimer previously suggested[25] is found to be an energy minimum by a vibrational analysis, and it lies 0.035 eV/BH_3 higher in energy than the C_{3v} trimer. In the previous study, one imaginary mode was found for such a C_2 trimer, and this was attributed to a lower SCF/DZP level of theory employed.[25]

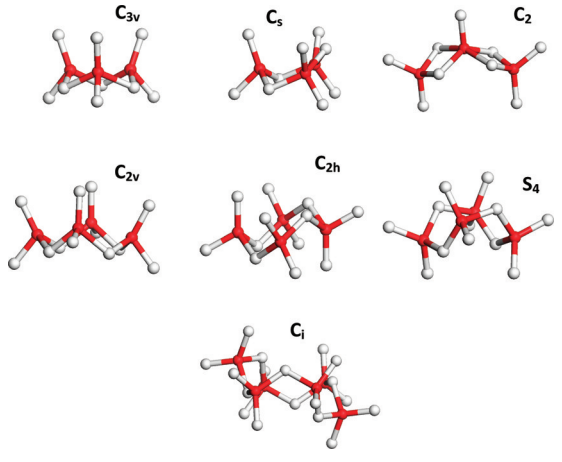

Figure 2. Preferred structures of trimers (three isomers, C_{3v}, C_s, and C_2), tetramers (three conformations, C_{2v}, C_{2h}, and S_4) and hexamer (C_i) of BH_3.

The B_4H_{12} tetramer has been previously studied, and a cyclic C_{2v} structure has been suggested as the local energy minimum.[27] This is what we find as well. The C_{2v} structure has a slightly puckered plane of B atoms, with all bridging H atoms on the same side of the plane (Figure 2). A more symmetrical C_{4v} structure is a saddle point (though not much higher in energy, +0.02 eV/BH_3 at CCSD(T)/cc-pVTZ level), distorting spontaneously to the C_{2v} minimum. In addition, we found two new isomers, C_{2h} and S_4, both having slightly lower energy than the C_{2v} structure. The C_{2h} structure has all B atoms in a plane, with bridging H atoms in an *aabb* pattern, where *a* = above, *b* = below the plane of the borons. The S_4 isomer has a puckered B arrangement, bridging hydrogens in an *abab* pattern. The energies of the C_{2h} and S_4 minima are 0.026 and 0.024 eV/BH_3 lower than that of the C_{2v} structure, respectively (at CCSD(T)/cc-pVTZ level, see SI to this paper). All tetramers are less stable per BH_3 than both the C_{3v} trimer and D_{2h} dimer.

We predict a C_i symmetry energy minimum structure for the B_6H_{18} hexamer. The C_i structure is slightly distorted from an idealized S_6 structure. In the C_i structure, the B atoms adopt a chair conformation and bridging H atoms are placed alternatively above and below the three planes (*ababab*, Figure 2). By rearranging the positions of H atoms in the C_i structure while keeping the basic chair conformation, several other structural variants are reached, all at higher energy. The C_i hexamer is less stable per BH_3 than the trimers, but slightly more stable than the tetramers.

Of course, other ring structures (5, 7, 8, etc.) are possible. These we did not examine. But we did look at the infinite chain, the limit of a large ring. In this, we were encouraged by our finding of such a geometry being important in a study of B_2I_6 under pressure.[28] We began with a simple chain with linear B–H–B linkages, shown at the top in Figure 3. We quickly found

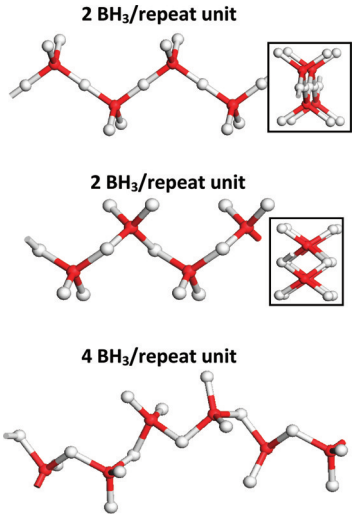

Figure 3. Structures of infinite 1-D chains.

dx.doi.org/10.1021/ja2092568 | J. Am. Chem.Soc. 2011, 133, 21002–21009

that this chain very much preferred to bend or kink at the H (by 0.267 eV/BH_3, using periodic DFT/GGA calculations), leading to the optimum structure at middle in Figure 3. We also constructed and examined several chains with four BH_3 units per repeat unit. The most stable chain with four BH_3's per repeat unit (bottom of Figure 3) is 0.005 eV/BH_3 higher in energy than the zigzag chain with two BH_3's per repeat unit (Figure 3, middle).

Bending at the Bridging Hydrogen Atom. A common feature in the molecules and chains described above is the presence of bent B−H−B bonds. The preference for a bent structure of some bridged electron-deficient molecules has been observed before. For example, the $B_2H_7^-$ anion also adopts

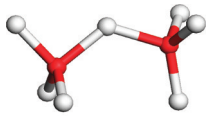

6

(experimentally and theoretically) a bent B−H−B linkage,[29,30] **6**.

Why does this bending occur? The explanation given[29,30] is that an "open" three-center two-electron bond, **7**, is less stable than a "closed" one, **8**, such as one has in these molecules. The argument goes back to the prototype for this kind of bonding, H_3^+, which clearly prefers equilateral triangle geometry to a linear one. Another way to express this preference is to say there is some BB bonding in an open three-center B−H−B bond. In contrast, the $Al_2H_7^-$ anion has a linear Al−H−Al linkage;[31,32] here the explanation given (not entirely convincing to us) is that there is now Al−Al repulsion, since the metallicity increases as one descends Group 13 in the periodic table.

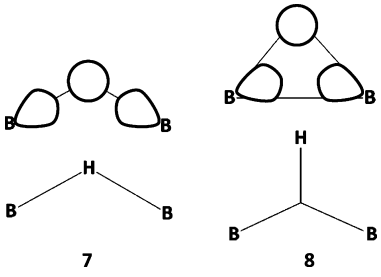

The Energies of Various $(BH_3)_n$ Structures Under Ambient Conditions. Figure 4 shows in one graph the relative energies (per BH_3) of the various isomers described above (at CCSD(T)/cc-pVTZ level). Diborane is the most stable form of $(BH_3)_n$ at ambient pressure; as we will see, this will not be true as the pressure is raised. The other structures, discussed in the preceding section, are not that much higher in energy and are all local minima.

A word here about the energy of the monomer, BH_3, which is at +1.01 eV in Figure 4: The oligomers calculated, except the monomer, have similar bonding patterns and therefore their zero-point energies (ZPE) are very close to each other (at MP2/cc-pVTZ level, calculated from the harmonic vibrational frequencies). The monomer, on the other hand has a lowered ZPE (SI to this paper). Including the ZPE contribution (−6.78 kcal/mol), the dissociation energy of diborane (to 2 BH_3) is about 39.9 kcal/mol ($T \rightarrow 0$ K). This is close to the measured dissociation enthalpy,[33] about 36 ± 3 kcal/mol, around 450 K, and generally agrees with previous theoretical calculations.[34]

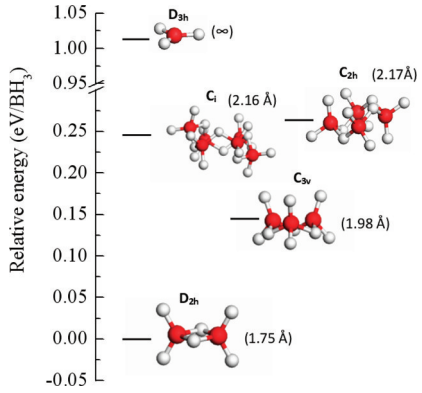

Figure 4. Calculated energies (see text for method, diborane is the reference) of the BH_3 monomer, dimer, trimer, tetramer, and hexamer. The symmetry and shortest BB distance (Å) are indicated for each.

For the zigzag chain, the periodic DFT/GGA calculations showed that its energy is in-between the energies of isolated C_{3v} trimer and C_i hexamer, which on the scale of Figure 4 is at 0.19 eV. We do not include its energy directly in Figure 4, since different methods were used for calculations of the oligomers (molecular programs) and the polymer (plane-wave extended structure programs). We have not studied the mechanisms for the hypothetical transformation of these oligomers to the more stable diborane or the associated activation energies.

In Figure 4, we indicate the optimized shortest BB separations in these isomers. Note the rough correlation with stability; clearly there is something to be gained in these systems from getting the borons closer together.

The BH = C Analogy. Another way to look at the molecular structures in Figure 4 is to implement an isolobal analogy, by replacing BH by C. Thus, the cyclic dimer, trimer, tetramer, hexamer, and 1-D infinite chain BH_3 are isoelectronic and isostructural to ethylene (C_2H_4), cyclopropane (C_3H_6), cyclobutane (C_4H_8), cyclohexane (C_6H_{12}), and polyethylene, respectively. It is amusing to probe this analogy, which actually served us to think of possible borane oligomer structures, a little further. This is done in the SI to this paper, using an electron localization function (ELF) analysis.[35]

The present study of B_2H_6 focuses on crystalline phases, omitting amorphous structures, only because we have no good way of studying them. To construct candidate extended structures of B_2H_6, we began with the molecular models described above, which are then stacked in different space group arrangements and optimized in the range of 1 atm to 100 GPa. The details of our calculations are given in the Methods section.

Crystalline Structures at High Pressures: Experiment. In recent spectroscopic experiments,[5] gaseous diborane was compressed up to 50 GPa, with three crystalline phases, named as I, II, and III, suggested in this pressure range. In these studies, the B_2H_6 gas was pressurized in a precooled (in liquid nitrogen) diamond anvil cell and then equilibrated to room temperature for the spectroscopic measurements. Both IR and Raman spectra were measured, at different pressures, and the appearances of new structures detected by spectroscopic changes upon pressurization. The B_2H_6 gas liquified below 4 GPa. It (recall that the melting point of diborane is 108 K) solidified into phase I around 4 GPa, transformed to phase II near 6.4 GPa, and then changed further, to a phase III near 14 GPa. These phase transitions are completely reversible on

dx.doi.org/10.1021/ja2092568 | J. Am. Chem.Soc. 2011, 133, 21002–21009

releasing pressures. No structural studies, that is, X-ray or neutron diffraction measurements, have been carried out on these phases.

Diborane under Pressure from 1 atm to 100 GPa: Dimers to Trimers to Polymers. We showed earlier the various diborane phases considered. Of these, we took the β form to higher pressure and compared its enthalpy to those of extended arrays of molecular trimer, tetramer, hexamer, and infinite chain of BH_3. The optimized structures we found (at 40 GPa) are shown in Figure 5, and their enthalpies as a function

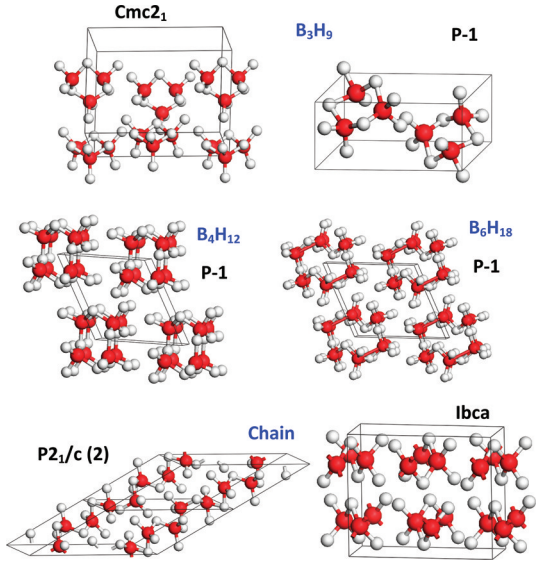

Figure 5. Molecular crystals constructed from the BH_3 trimer, tetramer, hexamer, and 1-D infinite chains.

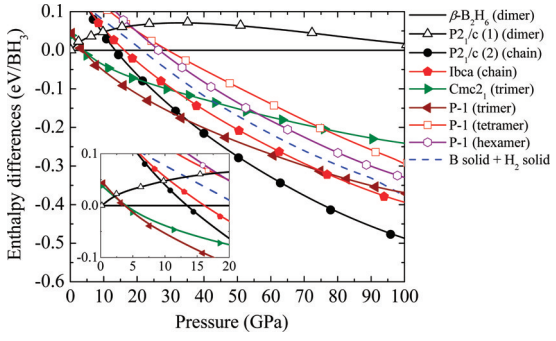

Figure 6. Calculated pressure dependences of enthalpies for selected high-pressure structures, relative to the β diborane structure.

of pressure in Figure 6. The reference zero is the β diborane structure. The enthalpies of the elements are also shown in Figure 6 by a dashed line. Here the α-B_{12}, γ-B_{28}, and α-Ga phases[36] are used for B, and the $P6_3/m$ and $C2/c$ phases[37] for H_2, in their appropriate pressure ranges.

The first thing to say is that as the pressure increases, very quickly a number of phases emerge as more stable than the reference β diborane (horizontal black line in Figure 6) of, for that matter, any diborane-type structure. Second, in the pressure range studied, all the phases retained their molecular identity. This is not true at higher pressures than those we studied, for in the work of Abe and Ashcroft,[7] for $P > 100$ GPa, new arrays of BH_3 composition come into play. Third, the tetramer and hexamer structures are never competitive, so we will not discuss them further. Fourth, in the pressure range covered, most phases are stable with respect to decomposition to the elements.

There is a worrisome apparent discrepancy in our calculations: We calculate the elements less stable than the β diborane structure by 0.37 eV per diborane molecule at $P = 1$ atm. But experimentally the heat of formation of diborane is positive by 0.38 eV.[38] ΔH_f^0 is under standard conditions, $T = 298$ K, while our calculations are for the ground state of the molecules, $T = 0$ K. In the SI, we show the effect of taking ΔH_f^0 to 0 K using experimental data.[39] That brings the experimental value for the formation reaction at 0 K down to 0.32 eV. In all the experimental estimates, the old problem of what is the most stable phases of boron, α or β, is a major uncertainty; the scope of the problem has been recently reviewed by Parakhonskiy et al.[40] It is not at all clear on which B allotrope the existing literature thermochemical measurements were made. Our calculations as quoted in this paper (Figure 6) do not include ZPE. When these are included, the elements become more stable than the β diborane structure by 0.27 eV per diborane molecule at $P = 1$ atm (calculated ZPE is solids: 0.13 eV/B,[41] 0.26 eV/H_2, 1.68 eV/B_2H_6), in a general agreement with the experimental heat of formation.

Near 4 GPa two trimer crystals, made up of distinct molecular B_3H_9 cyclic trimers, crystallizing in space group $Cmc2_1$ and P-1, become more stable than the β diborane.[42] Compression, even if slight, has an effect on the molecular geometry; the trimers in these two crystals distort slightly from the ideal calculated C_{3v} gas-phase structure. The stacking in these two structures differs notably in the orientation of the boron planes (Figure 5). There are two groups of boron planes in the $Cmc2_1$ structure that are almost normal to each other, while in the P-1 structure all boron planes are lined up. The $Cmc2_1$ structure has a permanent dipole moment. At higher pressure, the P-1 structure becomes increasingly more stable than the $Cmc2_1$ structure and is the lowest enthalpy phase until 36 GPa. The calculated phonon dispersion for the P-1 structure at 22 GPa (SI to this paper) shows no imaginary frequencies, indicating the structure is dynamically stable. The crystals built up from the more open pentacoordinated C_2 trimers are not competitive in this pressure regime.

Might the observed phase II of diborane[5] be one of the trimer structures, $Cmc2_1$ or P-1? The experiments were done at room temperature, the calculations at $T \rightarrow 0$ K. If the melting point of diborane increases with pressure, as is likely, phase I could be a crystalline diborane-like phase, such as the β phase or one of the other polymorphs we mentioned. The predicted dimer−trimer transition near 4 GPa is definitely a possibility for the phase I to II transition.

It could also be that phase II remains diborane-like, but has a large kinetic barrier to rearrangement to the more stable trimer phase we calculate. To get to a trimer, one would likely need to break down a dimer, a costly step in enthalpy, which has nevertheless been suggested[43] in the pyrolysis of B_2H_6 to yield higher boranes, that is,

$$B_2H_6 \rightleftharpoons 2\{BH_3\}$$
$$\{BH_3\} + B_2H_6 \rightleftharpoons \{B_3H_9\}$$

The measured dissociation enthalpy for step I is about 36 ± 3 kcal/mol (around 450 K).[33] Step II, the formation of a B_3H_9

dx.doi.org/10.1021/ja2092568 | J. Am. Chem.Soc. 2011, 133, 21002–21009

trimer, has not been unambiguously characterized in experiments. Fridmann and Fehlner[44] observed the formation of a triborane product, suggested to be B_3H_9, in the reaction of BH_3 and B_2H_6. Theoretical calculations[45] suggested that the step II is associated with activation and reaction enthalpies (at 400 K) of approximately 14 and −5 kcal/mol, respectively. It is not clear what the effect of increasing pressure would be on the activation energies for dimers transforming into trimers.

Finally, we might mention that we also tried a variety of other extended structures. One was based on extending the "pentacoordinated" trimer motif (see the C_2 structure of Figure 2) in two dimensions, a square net of B atoms, bridged along each edge of the square, with terminal hydrogen alternately above and below the plane. We found that this two-dimension sheet is unstable and distorts spontaneously to a layer of zigzag chains (Figure 3, middle). In the new layer, the basic square net of B atoms is kept. We have also built up trial crystal structures from these new layers; none were competitive. A second hypothetical structural alternative derived from the known AlH_3 geometry: a simple cubic lattice of B atoms bridged nonlinearly on every edge by hydrogens.[46] Barbee et al.[6] suggested that such an AlH_3-like BH_3 is more stable than the elements at high pressures, but in our calculations this phase has very high energy throughout the pressure range studied. A third hypothetical model adapted a recently predicted high-pressure GaH_3 structure.[47] Finally, Abe and Ashcroft suggested that another $P2_1/c$ structure might be the lowest-enthalpy phase for diborane between ambient pressure and 40 GPa.[7] This $P2_1/c$ structure, however, turns out in our calculations not to be competitive at any pressure (see SI).

A Regime of Linear Polymers for $(BH_3)_n$. Above 36 GPa, an extended structure constructed from 1-D chains of BH_3 stoichiometry becomes in our calculations the most stable phase and remains so to at least 100 GPa, the highest pressure studied in the present work. These chains have a periodic unit containing four BH_2 units linked by the bridging H atoms.

It might seem a coincidence that this structure shares the $P2_1/c$ space group with the β phase of molecular diborane, denoted as $P2_1/c$ (2) (Figures 5 and 6). But this is not an accident: the $P2_1/c$ (2) structure and the β diborane structure are closely related. Figure 7 shows the relationship.

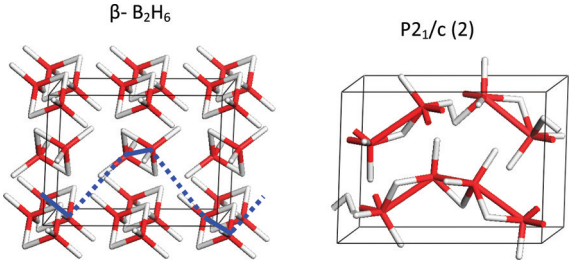

Figure 7. Structural interconversion between (left) the β diborane structure and (right) the $P2_1/c$ (2) structure. Dashed lines highlight the traces in the molecular structures of the bonds that would complete the chain.

We probed this transition, and in fact came to it, by a MD study. The simulation is carried out with a collection of atoms constrained in a finite cell that is spatially extended using periodic boundary conditions. The dynamics of the atoms are determined by solving Newton's equations of motion, which are discretized in sufficiently small time steps (1 fs). The interatomic forces are defined by force fields, which can be described either by semiempirical potentials or can be obtained quantum mechanically. We employed a quantum-mechanical approach in our MD simulations, using the plane-wave/pseudopotential method within a DFT implementation. The details of the MD calculations are presented in the Methods section.

The MD simulations show that the $P2_1/c$ (2) structure and the β diborane structure actually interconvert by applying/releasing pressures (Figure 7). At 40 GPa, a supercell of β diborane was relaxed for 10 ps at room temperature (300K) using a NVT molecular dynamics simulation, and reached the $P2_1/c$ (2) structure after a full structural optimization. Structural changes in the supercell take place at the very beginning stage of the MD simulation. Facilitated by the thermal motions, the dimers connect end-to-end to their neighbors, and eventually form infinite chains (dashed lines, Figure 7). The shape of the chains in the $P2_1/c$ (2) structure clearly keeps a trace of the arrangement of dimers in the β phase. Each periodic unit in the chain is constructed from two distinct dimers. This structural transformation is completely reversible in our calculations; the $P2_1/c$ (2) structure would transform back to the β diborane structure once the pressure is released. A similar transformation occurs for another metastable chain structure, *Ibca*, shown in Figure 5. With details shown in the SI, this chain also relaxes without activation energy to a dimer structure at 1 atm.

Energetically, the $P2_1/c$ (2) structure is a good candidate structure for the measured high-pressure phase III. It is also dynamically stable in this pressure regime, as indicated by the absence of imaginary phonon frequencies (SI to this paper). The close relationship between the polymeric $P2_1/c$ (2) structure and the β diborane structure is also interesting. In the recent experiments,[5] phases I and III were found to possess same number of lattice modes in their Raman spectra, and have similar spectra in the lattice region. This was considered as an indication that phases I and III are structurally related. We feel that we cannot, however, reach a definite conclusion in this matter based on the spectroscopic data alone.

We should also mention that none of our preferred structures, over the entire pressure range studied, was calculated to be metallic. Band gaps remain large, ranging from 5.3 eV in β diborane at 1 atm, to 4.2 eV in the trimer structure at 40 GPa, to 3.3 eV in the crystal of chain structures at 100 GPa. Of course, the material eventually metallizes as the pressure is increased further, as the Abe and Ashcroft calculations show.[7]

Why Are Rings and Chains More Stable than Diborane at Elevated Pressures? As one looks at the enthalpies of all the structures as a function of pressure (Figure 6), it is clear that diborane itself, whatever its three-dimensional structures, loses out with increasing pressure, first to three-membered ring structures and eventually to the chain structures, of which $P2_1/c$ (2) is the most stable. Why does this happen? The answer has to be in the "compactness", the ability to yield a denser structure. In the SI, we show some histograms of BH and BB distances of diborane versus the polymer structure, at one typical pressure, 40 GPa. Nothing significant emerges in the BH distances. But as far as BB separations go, one thing is apparent from the beginning: each B in β diborane has one near neighbor (1.64 Å, which is reduced by only about 0.1 Å from the value at ambient pressure), and the next-near neighbor B's are relatively far away

dx.doi.org/10.1021/ja2092568 | J. Am. Chem.Soc. 2011, 133, 21002–21009

(2.83 Å and 3.0 Å, reduced by compression from $P = 1$ atm for sure, but not yet in the region of bonding). But in the $P2_1/c$ (2) polymer structure, each B has *two* nearest neighbor B's, at 1.83 Å at 40 GPa. The distance is a bonding one, not that different from the BB separation in diborane at 1 atm.

So, the advantage the chain has over diborane is that it has an extra neighboring B atom participating in bonding. Figure 8

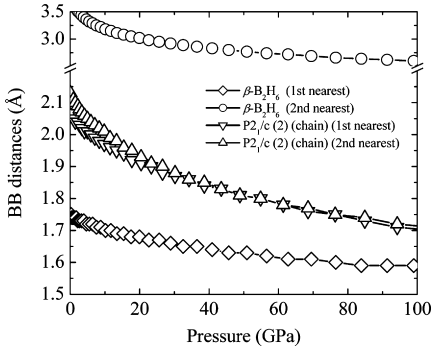

Figure 8. Pressure dependences of the first and second shortest BB distances in the $P2_1/c$ (2) chain structure and the β phase of diborane.

shows how this advantage is augmented with pressure; the two BB distances in the chain (the two curves with triangles) begin to approach the single shortest BB distance in β diborane (diamonds). Since the BH distances remain roughly constant, this correlation can also be expressed in another way, the BHB angles in the polymer chain (see Figure S8 in SI to this paper) decrease substantially with pressure, and approach the single BHB angle in β diborane.

What happens at still higher pressures? We refer the reader to the paper by Abe and Ashcroft,[7] which explores in detail structures above 100 GPa. This work shows that eventually higher density drives the system to more compact structures. The one-dimensional chains we find as most stable in the 40–100 GPa region lose out eventually, as one might expect, to still more compact extended 2D or/and 3D forms.

CONCLUSION

We have studied theoretically the molecular and crystalline structures of B_2H_6 in the pressure regime from 1 atm to 100 GPa. We found several metastable molecules, oligomers of BH_3, including trimer, tetramer, hexamer, and polymer structures; some of them are new. At 1 atm, we find a number of molecular diborane structures as most stable, all of them of comparable enthalpy. The structure known in atomic detail, β diborane, is reproduced. Three other diborane phases have been reported in the literature; one of our structures can reasonably explain the diffraction lines of the oldest of these, a crystalline phase reported in 1925 by Mark and Pohland. We have examined these diborane structures as the pressure increases, but also arrays of molecular trimers, tetramers, and hexamers of BH_3, as well as several infinite polymeric chains.

Near 4 GPa, a molecular crystal constructed from B_3H_9 trimers becomes the most stable phase. At 36 GPa, a phase built up of polymeric, one-dimensional chains replaces the trimer crystal to becomes the most stable phase and remains such until at least 100 GPa, the highest pressure studied in the present work. Phonon calculations showed that both predicted crystal structures are dynamically stable. The stabilities of the predicted structures are related to the bonding occurring between B atoms; they favor more compact structures with shorter BB contacts and/or higher B coordination.

ASSOCIATED CONTENT

Supporting Information

Details of computed energies for gas phase molecules; computed crystalline phase structural parameters; comparison between the simulated diffraction pattern of the $P2_1/c$ (1) structure and the measured pattern; ELF analysis for the B_3H_9 and C_3H_6 molecules; phonon dispersions for the P-1 (trimer) and $P2_1/c$ (2) structures; structural interconversion between the *Ibam* and *Ibca* structures; distance histograms for the β diborane structure and the $P2_1/c$ (2) structure; constructed molecular crystals with the frameworks of the B atoms demonstrated, enthalpy comparison between the P-1 (trimer), $P2_1/c$ (2) (chain), a previously predicted diborane structure, and an AlH_3-like BH_3 structure, pressure dependences of the BHB angles in the β diborane and $P2_1/c$ (2) chain structures; complete ref 19; an estimate of the heat of formation of diborane at 0K using experimental data. This material is available free of charge via the Internet at http://pubs.acs.org.

AUTHOR INFORMATION

Corresponding Author

rh34@cornell.edu

ACKNOWLEDGMENTS

Y.Y. is grateful to Dr. S. Patchkovskii for many helpful discussions on the quantum calculations and for critical reading and suggestions on the manuscript, and to Dr. D. D. Klug for help with the phonon calculations. We wish to thank Dr. T. P. Fehlner, Dr. K. Abe and Prof. N. W. Ashcroft for helpful discussions and communicating their results prior to publication. Our work at Cornell was supported by the National Science Foundation through Grant CHE-0910623.

REFERENCES

(1) Lipscomb, W. N. *Boron Hydrides*; Benjamin: New York, 1963.
(2) Rundle, R. E. *J. Am. Chem. Soc.* **1947**, *69*, 1327–1331.
(3) Pimentel, G. C. *J. Chem. Phys.* **1951**, *19*, 446–448.
(4) Pitzer, K. S. *J. Am. Chem. Soc.* **1945**, *67*, 1126–1132.
(5) Song, Y.; Murli, C.; Liu., Z. *J. Chem. Phys.* **2009**, *131*, 174506. Murli, C.; Song, Y. *J. Phys. Chem. B* **2009**, *113*, 13509–13515.
(6) Barbee, T. W. III; McMahan, A. K.; Klepeis, J. E.; Van Schilfgaarde, M. *Phys. Rev. B* **1997**, *56*, 5148–5155.
(7) Abe, K.; Ashcroft, N. W. *Phys. Rev. B.* **2011**, *84*, 104118.
(8) Mark, H.; Pohland, E. *Z. Kristallogr.* **1925**, *62*, 103–112.
(9) Bolz, L. H.; Mauer, F. A.; Peiser, H. S. *J. Chem. Phys.* **1959**, *31*, 1005–1007.
(10) Smith, H. W.; Lipscomb, W. N. *J. Chem. Phys.* **1965**, *43*, 1060–1064.
(11) Bartell, L. S.; Carroll, B. L. *J. Chem. Phys.* **1965**, *42*, 1135–1139. Hedberg, K.; Schomaker, V. *J. Am. Chem. Soc.* **1951**, *73*, 1482–1487. Bauer, S. H. *J. Am. Chem. Soc.* **1937**, *59*, 1096–1103.
(12) Price, W. C. *J. Chem. Phys.* **1948**, *16*, 894–902.
(13) Dunning, T. H. Jr. *J. Chem. Phys.* **1989**, *90*, 1007–1023.
(14) Bentz, J. L.; Olson, R. M.; Gordon, M. S.; Schmidt, M. W.; Kendall, R. A. *Comput. Phys. Commun.* **2007**, *176*, 589–600. Gordon, M. S.; Schmidt, M. W. In *Theory and Applications of Computational Chemistry, the First Forty Years*; Dykstra, C. E.; Frenking, G.; Kim, K. S.; Scuseria, G. E., Eds.; Elsevier: Amsterdam, 2005; pp 1167–1189. Piecuch, P.; Kucharski, S. A.; Kowalski, K.; Musial, M. *Comput. Phys. Commun.* **2002**, *149*, 71–96. Schmidt, M. W.; Baldridge, K. K.; Boatz, J. A.; Elbert, S. T.; Gordon, M. S.; Jensen, J. H.; Koseki, S.; Matsunaga,

N.; Nguyen, K. A.; Su, S.; Windus, T. L.; Dupuis, M.; Montgomery, J. A. *J. Comput. Chem.* **1993**, *14*, 1347−1363.
(15) Kresse, G.; Hafner, J. *Phys. Rev. B* **1993**, *47*, 558−561.
(16) Blöchl, P. E. *Phys. Rev. B* **1994**, *50*, 17953−17979. Kresse, G.; Joubert, D. *Phys. Rev. B* **1999**, *59*, 1758−1775.
(17) Perdew, J. P.; Burke, K.; Ernzerhof, M. *Phys. Rev. Lett.* **1997**, *78*, 1396−1396.
(18) Monkhorst, H. J.; Pack, J. D. *Phys. Rev. B* **1976**, *13*, 5188−5192.
(19) Gonze, X.; et al. *Comput. Mater. Sci.* **2002**, *25*, 478−492.
(20) Krack, M *Theor. Chem. Acc.* **2005**, *114*, 145−152. Troullier, N; Martins, J. *Phys. Rev. B* **1991**, *43*, 1993−2006.
(21) Greenwood, N. N.; Earnshaw, A. *Chemistry of elements*; Pergamon Press: Oxford, U.K., 1984.
(22) Grochala, W.; Hoffmann., R.; Feng, J.; Ashcroft, N. W. *Angew. Chem., Int. Ed.* **2007**, *46*, 3620−3642.
(23) Lipscomb, W. N.; McKee, M. L. *Inorg. Chem.* **1985**, *24*, 2317−2319.
(24) Stanton, J. F.; Lipscomb, W. N.; Bartlett, R. J.; McKee, M. L. *Inorg. Chem.* **1989**, *28*, 109−111.
(25) Duke, B. J.; Liang, C.; Schaefer, H. F. III. *J. Am. Chem. Soc.* **1991**, *113*, 2884−2890.
(26) Fehlner, T. P. *Boron Hydride Chemistry*; Muetterties, E. L., Ed.; Academic Press: New York, 1975; p 175.
(27) Shen, M.; Liang, C.; Schaefer, H. F. III. *Chem. Phys.* **1993**, *171*, 325−345.
(28) Yao, Y.; Klug, D. D.; Martoňák, R.; Patchkovskii, S. *Phys. Rev. B.* **2011**, *83*, 214105. Patchkovskii, S.; Klug, D. D.; Yao, Y. *Inorg. Chem.* **2011**, *50*, 10472−10475.
(29) Shore, S. G.; Lawrence, S. H. *J. Am. Chem. Soc.* **1982**, *104*, 7669−7670.
(30) Sapse, A. M.; Osorio, L. *Inorg. Chem.* **1984**, *23*, 627−628.
(31) Atwood, J. L.; Hrncir, D. C.; Rogers, R. D.; Howard, J. A. K. *J. Am. Chem. Soc.* **1981**, *103*, 6787−6788.
(32) Howell, J. M.; Sapse, A. M.; Sigman, E.; Snyder, G. *J. Am. Chem. Soc.* **1982**, *104*, 4758−4759.
(33) Fehlner, T. P.; Mappes, G W. *J. Phys. Chem.* **1969**, *73*, 873−882.
(34) Page, M.; Adams, G. F.; Binkley, J. S.; Melius, C. F. *J. Phys. Chem.* **1987**, *91*, 2675−2678. Stanton, J. F.; Bartlett, R. J.; Lipscomb, W. N. *Chem. Phys. Lett.* **1987**, *138*, 525−530. DeFrees, D. J.; Raghavachari, K.; Schlegel, H. B.; Pople, J. A.; Schleyer, P. v. R. *J. Phys. Chem.* **1987**, *91*, 1857−1864.
(35) Becke, A. D.; Edgecombe, K. E. *J. Chem. Phys.* **1990**, *92*, 5397−5403.
(36) Decker, B. F.; Kasper, J. S. *Acta Crystallogr.* **1959**, *12*, 503−506. Häussermann, U.; Simak, S. I.; Ahuja, R.; Johansson, B. *Phys. Rev. Lett.* **2003**, *90*, 065701. Oganov, A. R.; Chen, J. H.; Gatti, C.; Ma, Y. Z.; Ma, Y. M.; Glass, C. W.; Liu, Z. X.; Yu, T.; Kurakevych, O. O.; Solozhenko, V. L. *Nature (London)* **2009**, *457*, 863−867.
(37) Pickard, C. J.; Needs, R. J. *Nat. Phys.* **2007**, *3*, 473−476.
(38) Gurvich, L. V.; Veyts, I. V.; Alcock, C. B. *Thermodynamic Properties of Individual Substances*; fourth ed.; Hemisphere Pub. Co.: New York, 1989.
(39) Stitt, F. *J. Chem. Phys.* **1940**, *8*, 981−986. Johnston, H. L.; Clarke, J. T.; Rifkin, E. B.; Kerr, E. C. *J. Am. Chem. Soc.* **1950**, *72*, 3933−3938. Johnston, H. L.; Hersh, H. N.; Kerr, E. C. *J. Am. Chem. Soc.* **1951**, *73*, 1112−1117. Clarke, J. T.; Rifkin, E. B.; Johnston., H. L. *J. Am. Chem. Soc.* **1953**, *75*, 781−785. Ahlers, G. *J. Chem. Phys.* **1964**, *41*, 86−94. Krause, J. K.; Swenson, C. A. *Phys. Rev. B* **1980**, *21*, 2533−2548. McCarty, R. D.; Hord, J.; Roder, H. M. *Selected properties of Hydrogen (Engineering Design Data)*. *NBS Monograph 168*; U.S. Department of Commerce: Washington D.C., 1981; NIST Chemistry WebBook, http://webbook.nist.gov/chemistry/.
(40) Parakhonskiy, G.; Dubrovinskaia, N.; Bykova, E.; Wirth, R.; Dubrovinsky, L. *Sci. Rep.* **2011**, *1*, 96.
(41) Van Setten, M. J.; Uijttewal, M. A.; de Wijs, G. A.; de Groot, R. A. *J. Am. Chem. Soc.* **2007**, *129*, 2458−2465.
(42) The reader may note that the difference between the trimer and dimer structures at 1 atm in Figure 6 is about 0.05 eV/BH_3, less than the 0.144 eV/BH_3 shown for the molecules in Figure 4. We have simulated a molecular calculation with the VASP program used for the results in Figure 6, by placing molecules far apart (20 Å) from each other. The energy difference remains 0.05 eV. Thus, the discrepancy is due to either the differing accounting for correlations in the solid state (VASP) and molecular (GAMESS, CCSD(T)) calculations, or the inherent methodology (atom-centered basis functions for molecules, plane waves for the solid).
(43) Greenwood, N. N.; Greatrex, R. *Pure Appl. Chem.* **1987**, *59*, 857−868.
(44) Fridmann, S. A.; Fehlner, T. P. *J. Am. Chem. Soc.* **1971**, *93*, 2824−2826. Fridmann, S. A.; Fehlner, T. P. *Inorg. Chem.* **1972**, *11*, 936−940.
(45) Stanton, J. F.; Lipscomb, W. N.; Bartlett, R. J. *J. Am. Chem. Soc.* **1989**, *111*, 5165−5173.
(46) Turley, J. W.; Rinn, H. W. *Inorg. Chem.* **1969**, *8*, 18−22.
(47) Gao, G.; Wang, H.; Bergara, A.; Li, Y.; Liu, G.; Ma, Y. *Phys. Rev. B* **2011**, *84*, 064118.